A simple model for the evolution of melt pond coverage on permeable Arctic sea ice

Predrag Popović[1] and Dorian S. Abbot[1]

[1]Department of Geophysical sciences, University of Chicago, Hinds Geophysical Sciences, 5734 S. Ellis Ave., Chicago, IL 60637

Correspondence to: Predrag Popović (ppopovic@uchicago.edu)

Abstract.

As the melt season progresses, sea ice floes in the Arctic often become permeable enough to allow for nearly complete drainage of meltwater that has collected on the ice surface. Melt ponds that remain after drainage are hydraulically connected to the ocean, and correspond to regions of sea ice that are below sea level. We present a simple model for the evolution of melt pond coverage on such permeable sea ice floes, in which we allow for spatially varying ice melt rates and assume the whole floe is in hydrostatic balance. The model is represented by two simple ordinary differential equations, where the rate of change of pond coverage depends on the pond coverage, and all the physical parameters of the system are summarized by four strengths that control the relative importance of the terms in the equations. With this model, we are able to fit observations relatively well. Analysis of the model allows us to understand the behavior of melt ponds in a way that is often not possible using more complex models. We show that bare ice melting accounts for roughly half the pond growth, while melting ponded ice and ice bottom contribute less. Furthermore, our analysis demonstrates the somewhat surprising result that changes in bare ice albedo influence pond evolution roughly 5 times as much as corresponding changes in pond albedo. Performing a similar analysis, we estimate that under a global warming scenario, pond coverage would increase by at least 1.3% per Wm^{-2} per month. Using our model, we are able to extract the dependence of initial pond fraction, and show how melting different regions of the ice changes the pond coverage distribution differently. We also show that under certain conditions, ponds can stop growing. Since melt pond coverage is one of the key parameters controlling the albedo of sea ice, understanding the mechanisms that control the distribution of pond coverage will help improve large-scale model parameterizations and sea ice forecasts in a warming climate.

1 Introduction

Over the past forty years, Arctic summer sea ice extent has reduced by 50 percent, making it one of the most sensitive indicators of man-made climate change (Serreze and Stroeve, 2015; Stroeve et. al., 2007; Perovich and Richter-Menge, 2009). This rapid decrease is at least partially due to the ice-albedo feedback (Zhang et. al., 2008; Screen and Simmonds, 2010; Perovich et. al., 2007). Moreover,

if the ice-albedo feedback is strong enough it could lead to instabilities and abrupt changes in ice coverage in the future (North, 1984; Holland et. al., 2006; Eisenman and Wettlaufer, 2008; Abbot et al., 2011). The albedo of ice is strongly affected by the presence of melt ponds on its surface (Eicken et. al., 2004; Perovich and Polashenski, 2012; Yackel et. al., 2000). Therefore, understanding the evolution of melt ponds is essential for understanding the ice-albedo feedback, and consequently, the evolution of Arctic sea ice cover in a warming world. This means that accurate melt pond parameterizations must be incorporated into Global Climate Models (GCMs) to improve their sea ice forecasts (Flocco et. al., 2010; Holland et. al., 2012; Pedersen et. al., 2009). The main difficulties with including accurate melt pond parameterizations in large scale models are that pond evolution is nonlinear and that it is the result of a variety of different physical processes operating on a range of length and time scales. For these reasons, it is important to understand the mechanisms that drive the evolution of melt ponds.

Typically, the evolution of pond coverage on first-year ice proceeds in a fairly consistent manner (Polashenski et. al., 2012; Perovich et. al., 2003; Landy et. al., 2014; Webster et. al., 2015). First the ponds grow quickly while the ice is impermeable. Next they drain quickly and pond coverage shrinks as the ice transitions from impermeable to permeable. Then the ponds grow slowly while the ice is permeable and pond water remains at sea level. Finally, the ponds either refreeze or the floe breaks up. The stage when ice is highly permeable is typically the longest, sometimes lasting as long as the first two stages combined. This stage is particularly suitable to model, since the ponds can be assumed to be at sea level, and hydraulically connected to the ocean.

In this paper we will present a simple model for the evolution of melt pond coverage on sea ice floes. We will assume that ice is permeable, ponds are at sea level and hydraulically connected to the ocean, the whole ice floe is in hydrostatic balance, and different points on the ice surface may melt at different rates. Furthermore, we will assume that all the melt occurs either on the top surface or on the bottom surface of the ice, neglecting the possibility of ice melting internally. We will also neglect the possibility of pond growth by lateral melt of pond walls by the heat flux from the pond water. Nevertheless, we will discuss and assess the effects of both internal and lateral melt. The purpose of our model is: *i)* to clarify the roles played by physical parameters such as energy fluxes, the ice thickness, and initial pond coverage, in the evolution of pond coverage, *ii)* to provide a simple, yet accurate, way to estimate the pond coverage after a certain amount of time, *iii)* to understand the behavior of melt ponds under general environmental conditions, and *iv)* to investigate different types of qualitative behavior that can arise from differential melting and maintaining hydrostatic balance.

Skyllingstad et. al. (2009) also describe pond growth on permeable ice, but include only pond growth by lateral melt of pond walls. This contrasts with our model, which includes includes only pond growth by vertical changes of the topography (freeboard sinking and vertical sidewall melting). Our models are different, but complementary, and on several occasions we will draw parallels between our two models. Aside from Skyllingstad et. al. (2009), previous melt pond modeling ef-

forts include works by Taylor and Feltham (2004), Lüthje et. al. (2006), Scott and Feltham (2010), and Flocco and Feltham (2007), who all created comprehensive models that allowed for more realistic representations of physical processes such as heat and salt balance, and meltwater routing and drainage. The advantage of our model is its simplicity, and its analytical form, which makes it possible to clarify the roles of each of the physical parameters involved.

This paper is organized in the following way. In section 2 we build a simple model for the evolution of pond coverage. In section 3 we solve the model numerically using realistic parameters. In section 4 we analyze the model analytically to gain a better understanding of the factors influencing pond evolution. In section 5 we discuss: the physical processes that can change the rate of melt near the pond edge; lateral and internal melt; and the possibility of pond growth stopping. Finally in section 6 we summarize our results and conclude.

2 Building the simple model

In this section, we build the model for the evolution of melt pond coverage, and then solve it using realistic physical parameters. Before we proceed to build the quantitative model, we will first state the assumptions, and discuss the physical mechanisms driving pond evolution.

Our model focuses on the stage of pond evolution when ice is highly permeable and all the meltwater created is quickly removed to the ocean. The beginning of this stage can be identified as the point in time when pond coverage drops to its summer minimum, meaning that all the meltwater on the ice surface has drained to sea level, and the remaining ponds correspond to places on the ice surface that are below sea level. We will assume that from this point on, the ponds are hydraulically connected with the ocean, and the only way for pond coverage to increase is for the points on the ice surface which were above sea level to sink below sea level. In reality, ponds can also grow through horizontal melting of their sidewalls. As some observations suggest that this type of growth is small (Polashenski et. al., 2012; Landy et. al., 2014), we neglect it (see section 5.2 for further discussion). Furthermore, we will assume that all the melt occurs at the surface of the ice. We thereby neglect the possibility of internal melt, which we discuss in subsection 5.3. We will further assume that new ponds cannot form, and the only way for pond coverage to change is for existing ponds to change in size. Finally, we will assume that the entire ice floe is in hydrostatic balance.

The main goal of our model is to determine the fraction of the ice surface above sea level that falls below sea level after some time. Therefore, we focus on the vertical displacements of points on the surface of the ice in response to melt. To this end, we define the ice topography, $s(\boldsymbol{r})$, as the elevation of the ice surface above sea level at the point $\boldsymbol{r}$, and we define melt ponds as those regions where $s(\boldsymbol{r}) < 0$. There are two main reasons why the topography might change in response to ice melt:

a) First, the topography at a point $\boldsymbol{r}$ changes when ice at that point melts (Fig. 1 a). Here, the rate of change of topography at a point depends only on local characteristics of that particular point. For this reason, we will call this type of motion "local." Points on the surface in this way move "downwards," i.e. to lower elevations above sea level.

b) Second, in order to maintain hydrostatic balance, the entire ice surface can shift up or down in response to mass being removed above or below sea level. Since we are assuming that the entire ice floe is in hydrostatic balance, melting any region of ice moves the entire floe as a rigid body (Fig. 1 b). For this reason, we will call this type of motion the "rigid body" motion. An ice floe is not a rigid body, but up to its flexural wavelength we can approximate it as such. Melting above sea level induces an upward rigid body motion, whereas melting below sea level induces a downward rigid body motion.

At each point on the ice surface, the change in elevation above sea level can be calculated as the sum of these two contributions.

Since we are assuming that new ponds cannot form, the only way for pond coverage to change is through changes of topography near the pond boundaries. In our model, ponds grow in two ways:

a) Ponds can grow as a result of freeboard sinking. For points on bare ice, freeboard sinking represents a general downward shift of the non-changing topography as a result of overall thinning of the ice. Both rigid body movement and local melting contribute to freeboard sinking. Only the average local melt matters, since it determines the mass lost above sea level, and does not change the overall shape of the topography.

b) The other way ponds can grow is if the topography changes shape without changing its average height. Ponds can grow in this way if some regions melt faster than average. Therefore, a positive deviation in the local melt rate can grow ponds. Since we assume that no new ponds can form, pond growth by this mechanism is restricted to ice around the pond edge. Therefore, if the points near the pond boundaries melt at a faster rate than average, thereby changing the topography near the pond boundary, ponds will grow by "vertical sidewall melting." Vertical sidewall melting should not be confused with horizontal sidewall melting, (i.e. lateral melting) which we neglect. Vertical sidewall melting here represents a vertical motion of the ice surface near the pond boundary as a result of a deviation of the local melt rate from the average and not the horizontal motion of pond walls possibly induced by the lateral heat flux from the pond water.

For vertical sidewall melting to be significant, ice near the boundaries needs to, on average, have different properties than bare ice far away from the ponds. In fact, bare ice near the boundaries of the ponds is unique for at least two reasons: *i)* it is near sea level and *ii)* it is located at the ice-water interface. This special nature potentially provides it with unique topographical, thermal, and optical

properties, which can influence its rate of melt. Deviations from the mean melt rate for points far away from the pond edges do not influence pond evolution, since points at the pond perimeter and points far away from the pond edges are correlated only through hydrostatic adjustment which is determined by the average melt rates above and below sea level. Because hydrostatic adjustment can move the entire floe upwards if there is enough mass removed above sea level, ponds can even shrink as a response to melt if ice near the pond perimeter melts slowly enough.

We now proceed to build the quantitative model of pond evolution. Following the above ideas, we divide the total rate of change of vertical position of the point $\boldsymbol{r}$ on the surface of the ice, $\frac{ds}{dt}(\boldsymbol{r})$, into a contribution from rigid body motion, $\frac{ds_{\text{rigid body}}}{dt}$, and a contribution from local melting, $\frac{ds_{\text{loc}}}{dt}(\boldsymbol{r})$,

$$\frac{ds}{dt}(\boldsymbol{r}) = \frac{ds_{\text{rigid body}}}{dt} + \frac{ds_{\text{loc}}}{dt}(\boldsymbol{r}) \,. \tag{1}$$

Ice above sea level must hydrostatically balance the ice below sea level. We can write this hydrostatic balance as

$$m_{\text{above s. l.}} = \frac{\rho_{\text{w}} - \rho_{\text{i}}}{\rho_{\text{w}}} m_{\text{below s. l.}} \,, \tag{2}$$

where $m_{\text{above s. l.}}$, and $m_{\text{below s. l.}}$ represent the mass of ice above and below sea level, and ρ_{w}, and ρ_{i} represent the densities of water and ice.

The mass above and below sea level can change either because the ice melts or because the floe moves as a rigid body, changing the proportion of ice above and below sea level. Therefore, differentiating Eq. (2) and splitting into melt and rigid body contributions, we find

$$dm^{\text{melt}}_{\text{above s. l.}} + dm^{\text{rigid body}}_{\text{above s. l.}} = \frac{\rho_{\text{w}} - \rho_{\text{i}}}{\rho_{\text{w}}} \left[dm^{\text{melt}}_{\text{below s. l.}} + dm^{\text{rigid body}}_{\text{below s. l.}} \right] , \tag{3}$$

where $dm^{\text{melt/rigid body}}_{\text{above/below s. l.}}$ represent changes in mass above and below sea level due to either ice melting or the entire floe floating up or down.

The mass melted above and below sea level after some time dt is

$$\begin{aligned} dm^{\text{melt}}_{\text{above s. l.}} &= -A_{\text{bi}} \frac{\overline{F}_{\text{bi}}}{l} dt \,, \\ dm^{\text{melt}}_{\text{below s. l.}} &= -A_{\text{mp}} \frac{\overline{F}_{\text{mp}}}{l} dt - A \frac{\overline{F}_{\text{bot}}}{l} dt \,, \end{aligned} \tag{4}$$

where $l = 334 \frac{\text{kJ}}{\text{kg}}$ is the latent heat of melting, $\overline{F}_{\text{bi}}$ is the total energy flux used for melting bare ice averaged over all the regions of bare ice, $\overline{F}_{\text{mp}}$ is the total energy flux used for melting ponded ice averaged over all the regions of ponded ice, $\overline{F}_{\text{bot}}$ is the total energy flux used for melting the ice bottom averaged over the ice bottom, A_{bi}, A_{mp}, and A are the area of bare ice, the area of melt ponds, and the area of the entire floe.

Since floating up or down does not change the total mass of the ice, mass changes above and below sea level due to rigid body motion are equal with an opposite sign, $dm^{\text{rigid body}}_{\text{above s. l.}} = -dm^{\text{rigid body}}_{\text{below s. l.}}$. We can express $dm^{\text{rigid body}}$ in terms of rigid body displacement of the floe as

$$\begin{aligned} dm^{\text{rigid body}}_{\text{above s. l.}} &= \rho_i A_{\text{bi}} ds_{\text{rigid body}} \,, \\ dm^{\text{rigid body}}_{\text{below s. l.}} &= -\rho_i A_{\text{bi}} ds_{\text{rigid body}} \,. \end{aligned} \tag{5}$$

Substituting Eqs. (4) and (5) into Eq. (3), solving for $ds_{\text{rigid body}}$, and differentiating with respect to time, we find the rate of change of surface topography due to rigid body motion as

$$\frac{ds_{\text{rigid body}}}{dt} = \left[\frac{\rho_{\text{i}}}{\rho_{\text{w}}}\frac{\overline{F}_{\text{bi}}}{l\rho_i}\right] - \left[\frac{\rho_{\text{w}}-\rho_{\text{i}}}{\rho_{\text{w}}}\frac{A_{\text{mp}}}{A_{bi}}\frac{\overline{F}_{\text{mp}}}{l\rho_i}\right] - \left[\frac{\rho_{\text{w}}-\rho_{\text{i}}}{\rho_{\text{w}}}\frac{A}{A_{\text{bi}}}\frac{\overline{F}_{\text{bot}}}{l\rho_i}\right] . \tag{6}$$

The three terms in large square brackets correspond to topography change due to bare ice melting, ponded ice melting, and ice bottom melting. Rigid body motion depends only on spatially averaged energy fluxes, which in turn depend on parameters such as the average insolation on the floe, the average albedo, and the average longwave, sensible, latent and bottom heat fluxes. If bare and ponded ice melt only from energy absorbed by the upper surface of the ice, the fluxes $\overline{F}_{\text{bi}}$, and $\overline{F}_{\text{mp}}$ can also be written in terms of albedo as:

$$\begin{aligned}\overline{F}_{\text{bi}} &= (1-\alpha_{\text{bi}})F_{\text{sol}} + F_{\text{r}} ,\\ \overline{F}_{\text{mp}} &= (1-\alpha_{\text{mp}})F_{\text{sol}} + F_{\text{r}} ,\end{aligned} \tag{7}$$

where α_{bi} and α_{mp} are the average albedos of bare and ponded ice, F_{sol} is the solar flux, and F_{r} is equal to the sum of net longwave, net sensible, and net latent heat fluxes.

Local displacement, ds_{loc}, quantifies how much the ice surface topography changes as a result of local melt. We can determine the local melt rate from $F_{\text{surf}}(\boldsymbol{r})$, the flux of energy used for melting the ice surface at a point $\boldsymbol{r}$

$$\frac{ds_{\text{loc}}}{dt}(\boldsymbol{r}) = -\frac{F_{\text{surf}}(\boldsymbol{r})}{l\rho_i} , \tag{8}$$

where the positive direction is defined as upwards. The local flux depends on parameters such as the local albedo, the local insolation, the local longwave, sensible and latent heat fluxes, and the angle between ice and incoming radiation at that point.

If all melt happened on the surface of the ice, then the flux $F_{\text{surf}}(\boldsymbol{r})$ averaged over all the points on the surface of the ice above sea level would have to equal $\overline{F}_{\text{bi}}$

$$< F_{\text{surf}}(\boldsymbol{r}) >= \overline{F}_{\text{bi}} , \tag{9}$$

where $< ... >$ represents averaging over all the points on bare ice. For this reason, we will parameterize the rate of local melting as

$$\frac{ds_{\text{loc}}}{dt}(\boldsymbol{r}) = -k(\boldsymbol{r})\frac{\overline{F}_{\text{bi}}}{l\rho_i} , \tag{10}$$

where $k(\boldsymbol{r})$ is a non-dimensional number that quantifies the deviation of the melt rate at the point $\boldsymbol{r}$ from the mean melt rate of bare ice surface, which depends on the detailed conditions of ice and its environment. The parameter k could be either greater than or less than one. Here we will take k to be constant in time, but in reality it need not be. Finally, according to Eq. (1) we add Eq. (6) and Eq. (10) to get the equation for the evolution of the bare ice topography. We express this in terms of melt

pond fraction, $x \equiv \frac{A_{\text{mp}}}{A}$

$$\frac{ds}{dt}(\boldsymbol{r}) = -\Big[(k(\boldsymbol{r})-1)\frac{\overline{F}_{\text{bi}}}{l\rho_i}\Big] - \\ -\Big[\frac{\rho_w-\rho_i}{\rho_w}\frac{1}{l\rho_i}\big(\overline{F}_{\text{bi}} + \frac{x}{1-x}\overline{F}_{\text{mp}} + \frac{1}{1-x}\overline{F}_{\text{bot}}\big)\Big] \,. \tag{11}$$

Here, we split the equation into two terms, enclosed by the square brackets. The first term represents the local deviation from the average surface melt rate, which changes the general shape of the topography while preserving its average height above sea level. The second term represents a global shift of the average elevation above sea level due to freeboard sinking.

Both terms in Eq. (11) contribute to pond growth. Since we assume new ponds cannot form, the first term, which represents the topographic change due to deviation from the mean melt rate, can only grow the ponds by melting the ice near their boundaries. For this reason, we will identify the first term with vertical sidewall melting. Far from the pond edge, only the average melt rate matters by changing the rate of freeboard sinking. Therefore, for the purposes of estimating the evolution of pond coverage, we will assume that $k(\boldsymbol{r}) = 1$ far away from the pond boundary on bare ice, and $k(\boldsymbol{r}) \neq 1$ close to the boundary. In particular, we will assume $k(\boldsymbol{r}) \neq 1$ closer than some distance d from the pond perimeter, and that $k(\boldsymbol{r})$ is only a function of the distance from the pond edge. It is important that this distance is small, such that area where $k \neq 1$ is small compared to the total area of bare ice, since averaged over all the points on bare ice k needs to equal one. This assumption is reasonable, since close to the pond boundaries ice-water interaction could alter the melt rate.

In this way, the topographic evolution equation can be split into two terms: vertical sidewall melting, and freeboard sinking:

$$\frac{ds}{dt} = \frac{ds_{\text{sm}}}{dt} + \frac{ds_{\text{fs}}}{dt} \,, \tag{12}$$

where $\frac{ds_{\text{sm}}}{dt}$, and $\frac{ds_{\text{fs}}}{dt}$ are contributions from vertical sidewall melting, and freeboard sinking, and correspond to the first and second term of Eq. (11). This equation describes changes of topography near the perimeter of the ponds.

We now need to relate the vertical displacements near the pond boundaries to the change in area of the melt ponds. To this end we define the hypsographic curve, $s(x_h)$, that relates the elevation above sea level, s, to the percent of ice surface below that elevation, x_h (Fig. 2). Such curves have been measured and reported on several occasions (e.g. Fig. 8 of Eicken et. al. (2004), or Fig. 8 of Landy et. al. (2014)). If the ice is highly permeable, the melt pond fraction, x, can be inferred from a hypsographic curve as the intersection of sea level with the curve. Since ponds are hydraulically connected with the ocean, the average freeboard height, h, depends on the pond fraction. The average freeboard height, h, can be expressed in terms of the ice thickness H and pond fraction as

$$h = \frac{\rho_w - \rho_i}{\rho_w}\frac{H}{1-x} \,. \tag{13}$$

Here, the average freeboard height is defined as the elevation of the ice surface above sea level averaged over all the points of bare ice. For two ice floes of the same thickness, the one with higher

pond coverage will also need to have a higher average freeboard in order to maintain hydrostatic balance. For this reason we cannot use the hypsographic curves measured in the field if we wish to initialize our model with a pond coverage different than the one we have observational data for. We can address this problem by changing the measured hypsographic curve in a controlled way, so as to preserve the general shape of the measured curve, while satisfying the requirement for hydrostatic equilibrium for a particular choice of initial pond fraction and ice thickness. To get the new hypsographic curve for a particular initial pond fraction, x_i, ice thickness, H, and average pond depth, d, we split the observed hypsographic curve into the part above sea level and the part below sea level. We then stretch/contract the above sea level part of the curve along the x-axis to get the desired initial pond fraction, and then rescale it along the y-axis to get a freeboard that hydrostatically balances a floe of chosen thickness. Since topography below sea level is not important for the evolution of pond coverage, we replace the below sea level part with a straight line that satisfies the requirement that the average pond depth is d. We show an example of a measured hypsographic curve in Fig. 2 a), and show how we modify the curve for different initial ice thickness and initial pond coverage in Fig. 2 b) and c). We note that initial pond fraction, x_i, corresponds to the pond fraction when ice first becomes permeable.

Throughout this paper we use measurements of the hypsographic curve made by Landy et. al. (2014) for June 25th of 2011. We believe that such a statistical description of the ice topography should be general enough across different ice types, however, more measurements of sea ice topography would be useful in characterizing the variability in hypsographic curves. Part of the hypsographic curve above sea level measured by Landy et. al. (2014) is relatively well fit with a tangent function, $s(x_h) = a\tan(bx_h + c) + d$ (Fig. 2 a), red line). This tangent function is determined by four fitting parameters. If the fit to such a tangent function holds for sea ice hypsographic curves in general, knowing initial pond coverage, ice thickness, and ice roughness, we can constrain three of these parameters.

In the case of pure freeboard sinking the overall shape of the hypsographic curve does not change as the ice melts, but rather the whole curve is shifted following a displacement of ds_{fs}. We can calculate the resulting change in pond coverage as

$$\frac{dx}{dt} = \frac{dx_h}{ds}(x)\frac{ds_{\text{fs}}}{dt} \,, \tag{14}$$

where ds_{fs} is the vertical displacement of the bare ice topography due to freeboard sinking (as determined by the second term in Eq. (11)), and $\frac{dx_h}{ds_{\text{fs}}}(x)$ is the change in pond fraction for a vertical shift of the ice surface of ds_{fs} when the pond fraction is equal to x. It is equal to the reciprocal of the derivative of the hypsographic curve, $s(x_h)$, evaluated at $x_h = x$. Substituting $\frac{ds_{\text{fs}}}{dt}$ from Eq. (11) we find

$$\frac{dx}{dt} = \frac{d\hat{x}_h}{d\hat{s}}(x)\Big[S_{\text{bi}} + S_{\text{mp}}\frac{\widehat{x}}{\widehat{1-x}} + S_{\text{bot}}\frac{1}{\widehat{1-x}}\Big] \,, \tag{15}$$

where $\widehat{x} \equiv \frac{x}{x_i}$, and $\widehat{1-x} \equiv \frac{1-x}{1-x_i}$ are pond and bare ice fraction normalized by initial pond and bare ice fraction, $\frac{d\hat{x}_h}{d\hat{s}}(x) \equiv \frac{h}{1-x_i}\frac{dx_h}{ds}(x)$ is a non-dimensional slope of a hypsographic curve, and we have defined the strengths of pond growth by freeboard sinking due to melting bare, ponded, and ice bottom, S_{bi}, S_{mp}, and S_{bot} as

$$
\begin{aligned}
S_{\text{bi}} &\equiv \frac{(1-x_i)^2\overline{F}_{\text{bi}}}{Hl\rho_i}\,, \\
S_{\text{mp}} &\equiv \frac{(1-x_i)x_i\overline{F}_{\text{mp}}}{Hl\rho_i}\,, \\
S_{\text{bot}} &\equiv \frac{(1-x_i)\overline{F}_{\text{bot}}}{Hl\rho_i}\,,
\end{aligned}
\tag{16}
$$

The non-dimensional factors $\widehat{x}$, $\widehat{1-x}$, and $\frac{d\hat{x}_h}{d\hat{s}}(x)$ are chosen to be of the order unity, so that S_{bi}, S_{mp}, and S_{bot} control the strengths of pond growth by melting bare ice, melting ponded ice, and melting ice bottom. Reciprocals of the strengths represent the timescales of the growth modes.

The set of parameters needed to describe pure freeboard sinking can be further reduced by rewriting Eq. (15) as

$$
\frac{dx}{dt} = \frac{d\hat{x}_h}{d\hat{s}}(x)\Big[S_1\frac{\widehat{x}}{\widehat{1-x}} + S_2\frac{1}{\widehat{1-x}}\Big]\,,
\tag{17}
$$

where $S_1 \equiv S_{\text{mp}} - x_i S_{\text{bi}}/(1-x_i)$ and $S_1 \equiv S_{\text{bot}} + S_{\text{bi}}/(1-x_i)$ represent a minimal set of parameters needed to describe pure freeboard sinking. However, these parameters do not have a clear physical interpretation, and we will henceforth focus only on S_{bi}, S_{mp}, and S_{bot}.

In the case of pure vertical sidewall melting, the hypsographic curve only changes close to the pond boundary. To determine the fraction of ice affected by vertical sidewall melting, we convert the distance from the pond boundary where there is a significant deviation of the melt rate from the average, d, to ice fraction, $\delta = d\frac{P}{A}$, where P is the total perimeter of the ponds, and A is the area of the floe. Although, in general, pond perimeter, P, is a function of pond fraction, we will approximate it as constant. Let us now assume that the melt rate is only a function of distance from the pond edge, meaning that $k = k(x_h)$, and $k(x_h > x+\delta) \equiv 1$, and $k(x+\delta > x_h > x) \equiv k > 1$, where k is a constant larger than 1. If there is no topographic variation above sea level, and the entire ice floe above sea level has the same height, h, the pond coverage would grow by δ after a time $\Delta t = \frac{h}{ds_{\text{sm}}/dt}$. Therefore, the pond growth rate in this case would be $\frac{\Delta x}{\Delta t} = \frac{\delta}{h}\frac{ds_{\text{sm}}}{dt}$, where ds_{sm} is the vertical displacement of ice topography as determined by the first term of Eq. (11). If there is non-negligible topography above sea level described by the hypsographic curve, the time Δt it takes for pond coverage to grow by δ, would be $\Delta t = \frac{s(x_h = x+\delta)}{ds_{\text{sm}}/dt}$. Here, $s(x_h = x+\delta)$ is the original hypsographic curve evaluated at $x_h = x+\delta$. We will assume this expression generally holds for vertical sidewall melting. Thus, we arrive at the expression for pond growth due to pure vertical sidewall melting

$$
\frac{dx}{dt} = \frac{\delta}{s(x+\delta)}\frac{ds_{\text{sm}}}{dt}\,.
\tag{18}
$$

If δ is small compared to variation in the hypsographic curve, we can substitute $s(x+\delta)$ with $s(x)$. This is only not justified near the beginning of the melt, when $s(x) \approx 0$. We have made a number of assumptions in deriving the expression for vertical sidewall melting, such as assuming that $k(x_h)$ has a constant value larger than 1, and then suddenly drops to 1. Below we show that these assumptions are justified. Substituting $\frac{ds_{\text{sm}}}{dt}$ from Eq. (11) we find

$$\frac{dx}{dt} = S_{\text{sm}} \frac{1}{\hat{s}(x+\delta)} \,, \tag{19}$$

where $\hat{s}(x) \equiv \frac{s(x)}{h}$ is the non-dimensional hypsographic curve, and the strength of the vertical sidewall melting, S_{sm}, is defined as

$$S_{\text{sm}} \equiv \frac{\rho_{\text{w}}}{\rho_{\text{w}} - \rho_{\text{i}}} \frac{(1-x_i)\delta(k-1)\overline{F}_{\text{bi}}}{Hl\rho_i} \,, \tag{20}$$

Below we show that if the function describing the local melt rate, $k(x_h)$, has a non-trivial dependence on the distance from the pond boundary (or equivalently on x_h), the combination $\delta(k-1)$ is better replaced with a parameter $K \equiv \int_{x_i}^{1} (k(x_h) - 1) dx_h$.

Finally, we need to estimate pond coverage evolution when both freeboard sinking and vertical sidewall melting are happening simultaneously. We will assume that in this case, contributions from each of these processes can be added independently. Therefore, we solve Eq. (15) for pure freeboard sinking, and Eq. (19) for pure vertical sidewall melting independently, and add them together to get the full evolution of pond coverage, $x(t)$:

$$x(t) = x_{\text{fs}}(t) + x_{\text{sm}}(t) - x_i \,, \tag{21}$$

where $x_{\text{fs}}(t)$, and $x_{\text{sm}}(t)$ are solutions to Eq. (15), and Eq. (19), both forced using the same parameters, and initialized with the same initial pond fraction x_i.

In order to test the assumption of adding the two contributions independently, we have developed a "1D" model in which we explicitly determine pond evolution when both freeboard sinking and vertical sidewall melting are happening simultaneously. Apart from resolving the melt rates in one dimension, the underlying assumptions for the 1D model are essentially the same as for the simple model. For this reason, we simply give an outline for this model, without discussing it in much detail.

In the 1D model, we evolve the hypsographic curve by prescribing a melt rate, ds_{loc}, to each x_h depending on the distance from pond edge. The hypsographic curve above sea level far away from the pond edge melts at a uniform rate, whereas the hypsographic curve above sea level close to the pond edge melts at an enhanced rate. Parts of the curve below sea level melt at a uniform rate determined by the flux used for melting ponded ice, $\overline{F}_{\text{mp}}$. Finally, hydrostatic adjustment is calculated by finding the ice thickness directly at each time step, and placing the floe in hydrostatic balance. The evolution of pond coverage obtained from this model is shown in Fig. 3 a). The comparison with the simple model is excellent.

The 1D model allows us some freedom to test the detailed assumptions of the single column model. First, we can test how the functional form of $k(x_h)$ affects the pond evolution (Fig. 3 b). Functions $k(x_h)$ were chosen such that they all have the same integral parameter $K \equiv \int_{x_i}^{1}(k(x_h)-1)dx_h$. Figure 3 a) shows that in each of these cases the evolution of pond coverage proceeds nearly identically. Second, we can test the effects of varying pond albedo. In reality pond albedo decreases as the ponds deepen. We assume a dependence of pond albedo on pond depth by prescribing a constant pond bottom albedo and calculating the amount of sunlight absorbed by the pond water using the radiative properties of water presented in Table 1 of Skyllingstad et. al. (2009), and assuming this energy is used to melt ponded ice uniformly. The red dashed line in Fig. 3 a) shows that allowing for pond albedo to vary only has a small effect on pond evolution.

Equation (21) represents a sum of solutions to two simple ordinary differential equations, in which the rate of change of pond fraction depends on the pond fraction. Here, we have reduced the number of parameters from the original nine (H, x_i, $\overline{F}_{\text{bot}}$, F_{sol}, F_{r}, a_{bi}, a_{mp}, k, and δ) to four (S_{bi}, S_{mp}, S_{bot}, and S_{sm}). The strengths of freeboard sinking, S_{bi}, S_{mp}, and S_{bot}, depend only on the parameters that are available in GCM simulations, and are relatively easily measured in observational studies. The vertical sidewall melting strength, S_{sm}, however, also depends on the difficult-to-measure parameters k and δ that describe the melt rate near the pond boundary. If we could place some constraints on these parameters reliably enough, our model would be a useful parameterization in GCMs for pond growth after ice becomes permeable. Observations and detailed theoretical studies focusing on ice melt processes near the pond edge could constrain these parameters.

3 A simple model for the evolution of pond coverage can approximate observations using realistic parameters

We now solve Eq. (21) numerically using realistic values for the parameters. For shortwave, longwave, latent, and sensible heat fluxes, we use values inferred by Skyllingstad et. al. (2009) using hourly measurements from the SHEBA mission. We use the bottom heat flux inferred from measurements of ice bottom ablation during the SHEBA mission (Perovich et. al., 2003). The albedo of bare ice can vary between 0.5 and 0.7 (Hanesiak et. al., 2001), while the albedo of melt ponds can vary between 0.15 and 0.6, depending on pond depth and conditions of ice at the pond bottom (Perovich et. al., 2002b). Here we prescribe a default bare ice albedo of 0.6, and a default pond albedo of 0.4. Parameters k and δ depend on the physical mechanisms at play near the pond boundary such as bare ice wetting and washing away of dark particulates (see section 5). We can place some rough constraints on these parameters. We might expect that ice near the pond boundaries melts at some rate faster than bare ice, but slower than ponded ice. Using the average values of the fluxes and albedo, this puts k between 1 and $\frac{\overline{F}_{\text{mp}}}{\overline{F}_{\text{bi}}} \approx 1.67$. Here, we use $k = 1.2$. We can estimate δ from $\delta = d\frac{P}{A}$. From airborne photographs taken during the SHEBA mission, we find that late in the melt

season $\frac{P}{A} \approx 0.1$ m^{-1}. If we assume that there is significant interaction between ice and pond water at least 10 cm and at most 1 m from the pond edge, we find that δ lays between 0.01 and 0.1. Here, we use $\delta = 0.05$. This is clearly a rough estimate, but it is likely of the correct order of magnitude. We use an initial ice thickness of 2m, and use the topography measured by Landy et. al. (2014) adjusted for the prescribed ice thickness and initial pond fraction (usually $x_i = 0.2$). Although water and ice densities can vary due to changes in water salinity, internal ice melt, and the presence of air bubbles and brine in the ice, we will take these values to be fixed throughout the paper at $\rho_w = 1000\frac{\text{kg}}{\text{m}^3}$, and $\rho_i = 900\frac{\text{kg}}{\text{m}^3}$.

Figure 4 a) shows the solution to Eq. (21) for different initial conditions. We can see that ponds grow more rapidly when the initial pond coverage is lower, and the pond evolution curves cluster together as time progresses. This is because lower initial pond coverage corresponds to lower initial freeboard height, making the pond growth more rapid. The dashed line corresponds to the solution using the fluxes time-averaged over the 40 day run. The solutions using the averaged fluxes are very similar to the ones using time-varying fluxes, meaning that daily, and even monthly variations in the forcing have little effect on pond growth. Henceforth, we will use the time-averaged fluxes.

Larger ice thickness means a higher freeboard. For this reason, ponds grow more slowly on thicker ice. Because the pond growth rate is inversely proportional to ice thickness, $\frac{dx}{dt} \propto \frac{1}{H}$, pond coverage is more sensitive to variations in ice thickness when the ice is thin (4 b). In Fig. 4 b) we see that a 0.5m difference in the initial ice thickness (between a floe 1.5 m and a floe 2 m thick) can mean a 30% difference in pond coverage at the end of the melt season.

Figure 4 c) shows the dependence of pond coverage on albedo. A variation of 0.1 in bare ice albedo has a much larger effect on pond evolution than the same change in pond albedo. The reason is that melting ponded ice only affects pond coverage through downward rigid body motion of the floe, whereas melting bare ice grows the ponds through both vertical sidewall melting and freeboard sinking. Furthermore, rigid body motion due to ponded ice melting is proportional to the fraction of melt ponds, whereas freeboard sinking due to bare ice melting is independent of pond fraction.

The parameters k and δ are the least constrained parameters in our model. In Fig. 4 d) we show the dependence of pond evolution on the rate of melt near the pond boundary, k. Exploring the full range of realistic values for k, $1 < k < 1.6$, we find that the pond fraction at the end of the melt season can vary by about 20%. This difference would be larger if we chose a larger δ. If k is enough smaller than 1, S_{sm} can become negative, and the ponds can shrink. In this case, ice near the pond boundaries melts slowly enough such that an upward rigid body movement due to melting ice above sea level pushes the ice around the pond edge upwards. The evolution of shrinking ponds cannot be represented well in our model, and the blue curve in Fig. 4 d) serves therefore simply as an illustration.

The dotted line in Fig. 5 a) represents the solution to our model with flat topography using the full time-varying fluxes, ice thickness of 2 m, and vertical sidewall melting parameters $k = 1.5$,

and $\delta = 0.1$. When the topography above sea level is flat, freeboard sinking does not play a role in pond growth, while vertical sidewall melting does not depend on the pond fraction, and pond evolution becomes linear. As we discuss in below in subsection 5.2, assuming a flat topography above sea level, makes our model analogous to lateral melting. The red line on the same figure shows the results from the the lateral melting model of Skyllingstad et. al. (2009). Skyllingstad et. al. (2009) carefully calculated lateral melt rates from environmental conditions. The fact that the dotted line almost perfectly fits the results of Skyllingstad et. al. (2009) suggests that a single constant that relates the rate of melt of bare ice to the rate of melt of pond walls, K, is enough to capture the effects of lateral melting on pond growth. This suggests that the complicated physics of lateral melting can, to a large extent, be ignored. The dashed line represents the solution to our model using only vertical sidewall melting (only $S_{\text{sm}} \neq 0$) with non-flat topography. Including the topography significantly speeds up pond growth meaning that topography above sea level plays a large role in pond evolution. The solid black line represents the solution to the full Eq. (21), with both vertical sidewall melting and freeboard sinking included. The parameters k and δ are close to our limiting estimates, meaning that the vertical sidewall melting is strong and close to its upper limit. Even though vertical sidewall melting is strong, freeboard sinking accounts for nearly half the pond growth at the end of the melt season. This means that freeboard sinking should not be neglected even when vertical sidewall melting is strong.

In Fig. 5 b), we compare the results from our model to observations made on an albedo line during SHEBA. The full line represents a solution to the full Eq. (21). We use the melt rates of bare ice and ponded ice measured directly using ablation stakes during SHEBA (Perovich et. al., 2003). Since the ablation rates were measured directly, the ice thickness and the melt rate near the pond boundary are the only parameters left unconstrained. Knowing the ice thickness along the albedo line would make the strength of vertical sidewall melting, S_{sm}, the only fitting parameter. Unfortunately, no thickness measurements were made along the albedo line. A relatively good fit was obtained using realistic parameters $H = 1.6$ m, and $k = 1.5$. There is a noticeable discrepancy towards the end of the melt season. Since the measurements were made only along a 200 m albedo line, there could be a significant disagreement between the topography of the ice along the albedo line and the hypsographic curve we used, even if the topography of the entire floe corresponds well to the hypsographic curve we used. This difference in topography could explain the remaining discrepancy between the measurements and our model.

4 Analyzing the simple model yields useful insight into factors influencing the pond evolution

Extracting the dependence of a desired property on physical parameters and understanding its scaling is the main strength of our model. These types of relationships would be difficult to obtain in a more complex model.

The parameters S_{bi}, S_{mp}, S_{bot}, and S_{sm} control the rates of pond growth by melting different regions of ice. Roughly, they represent the amount of pond growth per unit time by freeboard sinking due to melting bare ice; freeboard sinking due to melting ponded ice; freeboard sinking due to melting ice bottom; and vertical sidewall melting. Analyzing these parameters can give useful insight into the behavior of melt ponds under general circumstances.

Different growth modes yield different pond evolution. Figure 6 shows phase portraits for pond fraction and solutions to Eq. (21) when only one of the strengths is non-zero. Common to all modes of growth is the dependence on ice thickness. Each growth mode is inversely proportional to the ice thickness, H, meaning that ponds grow proportionally slower on thicker ice.

The parameter S_{bi} is proportional to the flux $\overline{F}_{\text{bi}}$, and controls pond growth by freeboard sinking due to melting bare ice. This parameter becomes dominant if $\overline{F}_{\text{bi}}$ is high compared to the bottom melting flux, $\overline{F}_{\text{bot}}$, if initial pond coverage is small, and if k is close to one. Owing to the shape of the hypsographic curve, the pond growth rate by bare ice melting increases up to a certain pond coverage which lays roughly half-way between x_i and 1 and decreases afterwards (Fig. 6, blue line). S_{bi} depends on the initial pond coverage as $S_{\text{bi}} \propto (1-x_i)^2$. This means that ponds on floes with less initial pond coverage grow faster. The quadratic dependence on initial bare ice fraction also means that floes that start off less ponded can at some point become more ponded than floes that start off more heavily ponded. We can see this in Fig. 7 a), where the pond coverage distribution narrows up to a certain point, after which it starts to widen again because floes with lower x_i overtake the floes with higher x_i. Using the default values of physical parameters of $\overline{F}_{\text{bi}} = 73$ Wm^{-2}, $H = 2$ m, and $x_i = 0.2$, we get $S_{\text{bi}} \approx 0.2$ month^{-1}.

The parameter S_{mp} controls pond growth by freeboard sinking due to melting ponded ice. When $\overline{F}_{\text{mp}}$ is large compared to other fluxes and the initial pond coverage is high, this becomes the dominant mode of growth. The pond growth rate due to melting ponded ice increases with pond fraction (Fig. 6, green line). The dependence on initial pond coverage is $S_{\text{mp}} \propto x_i(1-x_i)$. For this reason the pond coverage distribution widens over time when S_{mp} is dominant (Fig. 7 b). Using $\overline{F}_{\text{mp}} = 122$ Wm^{-2}, we get $S_{\text{mp}} \approx 0.08$ month^{-1}.

The parameter S_{bot} controls pond growth by freeboard sinking due to melting of the ice bottom, and is dominant when $\overline{F}_{\text{bot}}$ is the dominant flux. The pond growth rate due to bottom melting increases with increasing melt pond fraction, although more gradually than in ponded ice melting case (Fig. 6, red line). Since the growth rate is proportional to the bare ice fraction, $S_{\text{bot}} \propto (1-x_i)$, the

pond coverage distribution gets concentrated over time (Fig. 7 c). Using $\overline{F}_{\text{bot}} = 20$ Wm^{-2}, we get $S_{\text{bot}} \approx 0.07$ month^{-1}.

The parameter S_{sm} controls pond growth by vertical sidewall melting, and is the least constrained in our model. It becomes dominant if $K = (k-1)\delta$ is large enough. Because the growth rate by vertical sidewall melting is inversely proportional to the hypsographic curve, pond growth by vertical sidewall melting is very fast at the beginning of the melt, and decelerates afterwards (Fig. 6, cyan line). Like bottom melting, vertical sidewall melting is also proportional to the bare ice fraction, $S_{\text{sm}} \propto (1 - x_i)$, meaning that the pond coverage distribution gets concentrated at the same rate as in the case of bottom melting (Fig. 7 d)). Since we cannot reliably estimate K, we can only place rough constraints on S_{sm}. If we assume that $1 \leq k \leq 1.67$, and that $0.01 \leq \delta \leq 0.1$, then $0 \leq K \leq 0.07$, and $0 \leq S_{\text{sm}} \leq 0.17$ month^{-1}. Even if S_{sm} is small, it can still have a significant effect, since near the beginning of the melt vertical sidewall melting is strong.

The black dashed line in Fig. 6 shows the total pond evolution using the default physical parameters. The evolution of the pond coverage distribution using the realistic parameters is shown in Fig. 7 e). The pond growth rate increases with increasing pond fraction, and the pond coverage distribution slowly narrows with time. Since each growth mode affects the pond coverage distribution in a distinct way, fitting both the evolution of the mean and the standard deviation of pond coverage distribution in observational data could add constraints on the relevant strengths. In the realistic simulation we used $k = 1.2$ and $\delta = 0.05$ which gives $S_{\text{sm}} \approx 0.025$ month^{-1}, roughly an order of magnitude less than S_{bi}. Using this value, we find that bare ice melting contributes to roughly 50% of pond growth, ponded ice and ice bottom melting both to around 20%, and vertical sidewall melting to roughly 10%. This would suggest that vertical sidewall melting is insignificant compared to freeboard sinking. Nevertheless, since vertical sidewall melting is strong at the beginning of the melt, it can still have a noticeable effect if the melt season is short enough.

We can use the strengths to estimate how pond evolution would be affected if the conditions were different. We can estimate the change in magnitude of the strength of each of the growth modes when a physical parameters p changes by Δp as

$$\Delta S_i = \frac{\partial S_i}{\partial p} \Delta p \,, \tag{22}$$

where ΔS_i is the change in magnitude of the strength of the ith growth mode. This equation holds so long as the change in the physical parameter is not too large. A change in pond growth rate can then be estimated as $\Delta R = \sum_i \Delta S_i$. We can roughly estimate a change in pond fraction, Δx, after some time, Δt, following a change in physical parameter, p, as $\Delta x \approx \Delta R \Delta t$. This provides a means to estimate changes in pond coverage under different environmental conditions without solving the model numerically.

We will illustrate this on an example of varying ice and pond albedo. If the bare ice albedo changes by $\Delta\alpha_{\text{bi}}$, the change in growth rate would be roughly

$$\Delta R = -\big[(1-x_i) + \frac{\rho_w}{\rho_w - \rho_i}(k-1)\delta\big]\frac{(1-x_i)F_{\text{sol}}}{Hl\rho_i}\Delta\alpha_{\text{bi}} \approx -0.75\frac{1}{\text{month}}\Delta\alpha_{\text{bi}}\ . \tag{23}$$

On the other hand, if the melt pond albedo changes by $\Delta\alpha_{\text{mp}}$, the first and third modes do not change, the change in growth rate would be roughly

$$\Delta R = -\frac{x_i(1-x_i)F_{\text{sol}}}{Hl\rho_i}\Delta\alpha_{\text{mp}} \approx -0.15\frac{1}{\text{month}}\Delta\alpha_{\text{mp}}\ . \tag{24}$$

The initial pond fraction used was $x_i = 0.2$. It follows from these estimates that after a month, the pond fraction would differ by roughly 7.5% for a bare ice albedo difference of 0.1, and by around 1.5% for a ponded ice albedo difference of 0.1. Therefore, variation in pond albedo affects pond evolution roughly 5 times less than variation in bare ice albedo. This explains our observation from Fig. 4 c) that pond evolution is much more sensitive to variation in bare ice albedo than to variation in pond albedo. In this way, we also extract the dependence of sensitivity on physical parameters. Therefore, we can see that the sensitivity to pond albedo is highest when pond coverage is 50%, and the sensitivity to bare ice albedo is highest when a floe is pond-free.

In the high latitudes, feedbacks due to changes in albedo, the atmospheric lapse rate, and clouds can amplify the forcing due to global warming (Holland and Bitz, 2006). For this reason forcing in the high latitudes is generally going to be larger than direct radiative forcing due to an increase in CO_2 concentration. In a global warming scenario, pond growth rate would increase because the ice melts faster, but also the because ice at the beginning of the melt would be thinner. We can emulate a global warming scenario by increasing the flux F_r by a certain amount, ΔF_r, and by assuming that the initial ice thickness decreases by $\Delta H \equiv \frac{\partial H}{\partial F_r}\Delta F_r$, where $\frac{\partial H}{\partial F_r}$ is the ice thinning per $1\ \text{Wm}^{-2}$ of warming. Therefore, we split the change in pond growth rate due to global warming, ΔR, into a contribution from direct forcing, ΔR_F, and a contribution from ice thinning, ΔR_H. Using the above formalism, we find that

$$\begin{aligned}
\Delta R_F &\equiv \sum_i \frac{\partial S_i}{\partial F_r}\Delta F_r = \big[1 + \frac{\rho_w}{\rho_w - \rho_i}(k-1)\delta\big]\frac{1-x_i}{Hl\rho_i}\Delta F_r \approx \frac{0.38\%}{\text{W/m}^2 \times \text{month}}\Delta F_r\ , \\
\Delta R_H &\equiv \sum_i \frac{\partial S_i}{\partial H}\frac{\partial H}{\partial F_r}\Delta F_r = -\big[S_{\text{bi}} + S_{\text{mp}} + S_{\text{bot}} + S_{\text{sm}}\big]\frac{1}{H}\frac{\partial H}{\partial F_r}\Delta F_r \approx \frac{0.96\%}{\text{W/m}^2 \times \text{month}}\Delta F_r\ , \\
\Delta R &\equiv \Delta R_F + \Delta R_H \approx \frac{1.34\%}{\text{W/m}^2 \times \text{month}}\Delta F_r\ .
\end{aligned} \tag{25}$$

The numbers in Eq (25) were obtained using the default values of the parameters, and $\frac{\partial H}{\partial F_r} = -0.05\ \text{m}^3\text{W}^{-1}$ roughly estimated using the Eisenman and Wettlaufer (2008) model. This means that after a month's growth global warming would increase pond coverage by roughly 1.3% per $1\ \text{Wm}^{-2}$ of warming. Simulating a 30 day melt numerically using our model predicts an increase in

pond coverage with forcing at a rate of 1.1% per 1 Wm^{-2} of warming for small forcing ($\Delta F_r \approx 0$), increasing up to 5.6% per 1 Wm^{-2} for large forcing ($\Delta F_r \approx 15$ Wm^{-2}). This convex dependence is due to increased sensitivity to forcing on thinner ice, and can be reproduced by evaluating ΔR at $F_r + \Delta F_r$ and $H + \frac{\partial H}{\partial F_r}\Delta F_r$. Our simple estimate, Eq. (25), which is only valid for small forcing, gives reasonable results without having to run numerical simulations. It also gives the dependence of sensitivity on physical parameters. Therefore pond coverage on thinner ice with less pond coverage is more sensitive to forcing. In a likely scenario where forcing is around 10 Wm^{-2}, our estimate predicts that after a month pond coverage would increase by around 13%. In a global warming scenario increased forcing could also lead changes in initial pond coverage or changes in K. We ignored these feedbacks, as we have no way of reliably estimating $\frac{\partial x_i}{\partial F_r}$ and $\frac{\partial K}{\partial F_r}$.

5 Discussion

5.1 Physical processes that influence the rate of melt near the pond boundary

Several mechanisms can accelerate ice melting near the boundaries of melt ponds:

a) Even a very thin layer of water on top of ice can significantly decrease its albedo due to the effect of multiple light reflections (Makshtas and Podgorny, 1996). Since pond water could wet the surrounding ice, this mechanism could lead to ice near the pond boundaries melting faster than bare ice far away from the ponds.

b) Wetting the ice surface can also decrease its albedo in another way. If the ice is rough and jagged on a small scale, it will have a high reflectance. Due to the effects of surface tension increasing the pressure, ice crystals with a small radius of curvature will be under higher pressure, and will therefore have a lower melting point than large flat crystals. If a collection of crystals of small but varying size is submerged in water that is at the crystals' mean melting temperature, small crystals will melt, and large crystals will grow at their expense through a process called Ostwald ripening (Raymond and Tusima, 1979). This process will smooth the ice, lowering its reflectiveness, and accelerating the rate of melt.

c) Bands of dark algae are often washed up on the perimeter of advanced ponds, accelerating the melting.

d) If all points on the surface of bare ice melt at similar rates that fluctuate slightly around the average, points near sea level would have a higher probability of falling below sea level through these random fluctuations. Ice that falls below sea level would become flooded and start melting faster, preventing it from returning to its previous position above sea level. Therefore, simply because they are closer to sea level, points near the pond boundary would effectively melt faster than points far away that have a higher elevation.

All of the above mechanisms that rely on decreasing the albedo will have a lesser effect if the conditions are cloudy. Even though we expect the pond boundary to melt faster than bare ice on average, there are some straightforward mechanisms that could cause a slower melt rate at the pond edge, and, under the right conditions, these could possibly even outweigh the accelerating mechanisms:

a) The diurnal cycle could be such that ice melts during some part of the day and freezes during another, with net melting occurring on average. Since ice is permeable, meltwater created during the melting part of the day above bare ice could seep through the ice. During the freezing part of the day, there would be no water to freeze on bare ice, but there would be an abundance of water at the pond edge which could freeze, thus making the net melting rate at the pond boundary lower than the average net melting rate on bare ice.

b) Arctic sea ice is often loaded with dark impurities, such as dust, black carbon or sediments (Nürnberg et. al., 1994; Pfirman et. al., 1990; Perovich et. al., 1998; Light et. al., 1998; Tucker et. al., 1999). Dark particulates can significantly lower the albedo of ice. If the ice has a significant amount of impurities, bare ice could stay covered in dirt, whereas water could wash away the dust on the edge of the ponds, exposing the more reflective white ice. In this way, the pond edge could have a lower albedo than the rest of the bare ice.

c) Pressure ridges correspond to regions of thick ice and pronounced topography. For this reason ridge sails can collect more sunlight, and melt faster than other regions on the ice surface. Therefore, ridges can enhance the average melt rate of bare ice compared to ice near the pond edge, effectively decreasing the melt rate of ice near the pond boundary.

As of yet, we do not have enough information to make a reliable estimate of vertical sidewall melting. However, studies by Landy et. al. (2014) and Polashenski et. al. (2012) suggest that ponds grow mostly by freeboard sinking, meaning that $K \approx 0$. These are, however, only two case studies of very limited spatial coverage. It would be best if more such observations were made in different regions of the Arctic, and under varying environmental conditions.

5.2 Lateral melting of pond walls by pond water

In our model, we focused on vertical changes of the topography, and neglected pond growth by lateral melting of pond sidewalls by pond water. We will now briefly discuss this possibility.

This type of melt was the main focus of Skyllingstad et. al. (2009), who carefully calculated the lateral melt rates of pond sidewalls by pond water. The rate of change of pond fraction due to a lateral melt flux $\overline{F}_{\text{lat}}$ is

$$\frac{dx_{\text{lat}}}{dt} = \frac{P}{A}\frac{\overline{F}_{\text{lat}}}{L}\,, \tag{26}$$

where P is the total perimeter of the ponds and A is the area of the floe. If $\overline{F}_{\text{lat}}$ is constant, pond growth is linear, which explains the the apparently linear pond coverage evolution in Skyllingstad et.

al. (2009). As we have suggested in section 3, lateral melt flux can likely be assumed proportional to the bare ice melting flux, $\overline{F}_{\text{lat}} = K_{\text{lat}}\overline{F}_{\text{bi}}$, where K_{lat} is a constant. It is important to note that lateral melt does not depend on ice thickness, H, or on initial pond coverage, x_i. Assuming a flat topography above sea level in our model makes vertical sidewall melting the only means of pond growth. In this case the pond growth rate is independent of pond fraction, and in that sense is analogous to lateral melting. Nevertheless, vertical sidewall melting with flat topography still depends on ice thickness and initial pond coverage.

When ponds grow by lateral melt, the growth rate is constant, and the growth is linear (Fig. 6, dashed magenta line). Furthermore, the pond growth rate does not depend on the ice thickness or on initial pond coverage. For this reason, the pond coverage distribution width does not change in time, while the mean increases linearly (Fig. 7 f).

Each point along the pond boundary can either expand by lateral melting or by vertical melting, but not by both. This is because when a point along the pond boundary melts laterally, it creates a completely vertical slope at that point. Therefore a small vertical shift will not grow the ponds, and a large vertical shift will outgrow the lateral expansion. Having this in mind, a potential model for pond evolution that includes both lateral, and vertical melt could read

$$x(t) = f x_{\text{vert}}(t) + (1-f)x_{\text{lat}}(t) - x_i \ . \tag{27}$$

where $x_{\text{vert}}(t)$ is the solution to our simple model (Eq. (21)), $x_{\text{lat}}(t)$ is the solution Eq. (26), and f is the fraction of the points on the ice surface that sink below sea level via vertical motions of the topography. It should be possible to estimate f observationally by observing the slope of ice at the pond boundaries. Regions of very steep topography along the pond boundaries should correspond to regions of lateral melt, whereas regions of growth by vertical melt should correspond to more gently sloped regions. Some field measurements indicate that ponds grow mostly by freeboard sinking (Polashenski et. al., 2012; Landy et. al., 2014), meaning that that f should be close to 1.

5.3 Internal melt

So far, we have assumed that all the melt occurs either on the top or the bottom surface of the ice. However, some of the melt can happen internally, in the bulk of the ice. Internal melt occurs when trapped brine pockets with high salt content expand and dilute in order to reach a thermodynamic equilibrium with the surrounding ice. This phenomenon has been reported to occur both above and below sea level. Accounting for internal melt correctly can be quite challenging as it requires detailed knowledge of the vertical structure of internal melt. For this reason, we do not include internal melt in our model, but only briefly discuss the qualitative effects.

Internal melt induces rigid body motion by melting mass above and below sea level, without changing the ice surface. It therefore only enters the pond evolution equation by changing the mass

lost above and below sea level, Eq (4)

$$dm^{\text{melt}}_{\text{above s. l.}} = -A_{\text{bi}}\frac{\overline{F}_{\text{bi}}}{l}dt - A_{\text{bi}}h\frac{\overline{e}_{\text{above s. l.}}}{l}dt$$
$$dm^{\text{melt}}_{\text{below s. l.}} = -A_{\text{mp}}\frac{\overline{F}_{\text{mp}}}{l}dt - A\frac{\overline{F}_{\text{bot}}}{l}dt - AH_d\frac{\overline{e}_{\text{below s. l.}}}{l}dt\,, \tag{28}$$

where $H_d = \frac{\rho_i}{\rho_w-\rho_i}h(1-x)$ is the ice draft depth defined as the volume of ice below sea level divided by the area of the ice floe, and $\overline{e}_{\text{above/below s. l.}}$ is the energy density used for internal melting, averaged over all ice above or below sea level. Here, the fluxes $\overline{F}_{\text{bi}}$, $\overline{F}_{\text{mp}}$, and $\overline{F}_{\text{bot}}$ represent energy fluxes used for melting the ice surface.

With this change, we can find the equation for pond coverage evolution straightforwardly, by repeating all of the steps from section 2. We first derive the equation for the vertical motion of points near the pond perimeter

$$\frac{ds}{dt} = -\Big[(k-1)\frac{\overline{F}_{\text{bi}}}{l\rho_i}\Big] -$$
$$-\Big[\frac{\rho_w-\rho_i}{\rho_w}\frac{1}{l\rho_i}\big(\overline{F}_{\text{bi}} + \frac{x}{1-x}\overline{F}_{\text{mp}} + \frac{1}{1-x}(\overline{F}_{\text{bot}} - \frac{\rho_i}{\rho_w}H\Delta e)\big)\Big]\,, \tag{29}$$

where $\Delta e \equiv \overline{e}_{\text{above s. l.}} - \overline{e}_{\text{below s. l.}}$ is the difference in average energy density used for internal melting above and below sea level, and the two terms in square brackets correspond to vertical sidewall melting and freeboard sinking. Then we repeat the procedure to relate Eq. (29) to the change in pond coverage. The resulting equation has the same form as Eq. (21), with only the strength of freeboard sinking due to ice bottom melting modified

$$S_{\text{bot}} \to S_{\text{bot+int}} \equiv \frac{(1-x_i)\Big(\overline{F}_{\text{bot}} - \frac{\rho_i}{\rho_w}H\Delta e\Big)}{Hl\rho_i}\,. \tag{30}$$

In the absence of internal melt, Eqs. (16), (20), (21), and (30) are enough to describe pond evolution. However, when internal melt occurs, another equation for evolution of bulk ice density is required. This requires a detailed knowledge of the vertical structure of internal melt, $e(z)$, which makes it too complicated to include in our model. We proceed to simply discuss the qualitative effects of internal melt. In this discussion, we assume z is increasing upwards.

a) If internal melt is uniform throughout the floe, the energy density difference above and below sea level is zero, $\Delta e = 0$. For this reason, internal melt has no effect on rigid body motion. The only effect of internal melt in this case is the reduction in ice density. This effect always accelerates pond growth.

b) If internal melt decreases with z, $\Delta e < 0$. Pond growth in this case is accelerated both by the effect of internal melt on freeboard, and by a reduction in density.

c) If internal melt increases with z, $\Delta e > 0$. In this case the freeboard effect of internal melt would decelerate pond growth, while the density effect would accelerate it. Internal melt,

therefore, could either accelerate or decelerate pond growth. At the beginning of the melt, the effect is always decelerating, since the bulk ice density has not had enough time to change substantially. However, if enough time passes, the density will have decreased enough to actually accelerate pond growth. If Δe is positive enough, pond growth can even be reversed, and the ponds can start shrinking.

5.4 Under certain conditions, ponds can stop growing

Equation (29) for the evolution of topography near the pond edge including effects of internal melt allows for $\frac{ds}{dt} > 0$, meaning that points near the pond perimeter can move upwards, so that ponds can stop growing, or even shrink. This happens when there is enough mass removed above sea level to induce an upward freeboard motion that is able to compensate for the effects of local melting near the pond edge.

The relationships between vertical displacement of a point near the pond perimeter and change in pond coverage are not captured well in our model when the displacement is upwards, meaning that it cannot accurately describe the pond shrinking scenario. Nevertheless, we can use Eq. (29) to find the exact condition for points near the pond boundary to move upwards. Setting $\frac{ds}{dt}(x) > 0$ for any x, we find

$$k < \frac{\rho_\mathrm{i}}{\rho_\mathrm{w}}\left(1 + \frac{h\Delta e}{\overline{F}_\mathrm{bi}}\right) - \frac{\rho_\mathrm{w} - \rho_\mathrm{i}}{\rho_\mathrm{w}}\frac{\overline{F}_\mathrm{bot}}{\overline{F}_\mathrm{bi}}\,, \tag{31}$$

where h is the initial freeboard height. If $k = 1$, the internal melt difference needs to be at least $h\Delta e > \frac{\rho_w - \rho_i}{\rho_i}\overline{F}_\mathrm{bot} \approx 2.2\frac{\mathrm{W}}{\mathrm{m}^2}$ in order to satisfy Eq. (31). If $\Delta e = 0$, k has to be less than 0.87 to to satisfy Eq. (31), that is, ice near the pond boundary needs to melt 13% slower than bare ice on average.

Condition Eq. (31) means that there exists at least some x for which the ponds shrink (or at least stop growing through vertical motions of the topography). Nevertheless, for high enough pond coverage ponds would still grow, since an upward rigid body motion due to melting bare ice would be insufficient to overcome the downward tendencies of melting ice below sea level. There exists a pond coverage, x_0, for which ponds neither shrink nor grow. We can find its value by requiring $\frac{ds}{dt}(x_0) = 0$

$$x_0 = \frac{(\frac{\rho_\mathrm{i}}{\rho_\mathrm{w}} - k)\overline{F}_\mathrm{bi} + \frac{\rho_i}{\rho_w}h\Delta e - \frac{\rho_\mathrm{w} - \rho_\mathrm{i}}{\rho_\mathrm{w}}\overline{F}_\mathrm{bot}}{(\frac{\rho_\mathrm{i}}{\rho_\mathrm{w}} - k)\overline{F}_\mathrm{bi} + \frac{\rho_i}{\rho_w}h\Delta e + \frac{\rho_\mathrm{w} - \rho_\mathrm{i}}{\rho_\mathrm{w}}\overline{F}_\mathrm{mp}}\,. \tag{32}$$

x_0 is a fixed point of the Eq. (21), and lays between 0 and 1 if Eq. (31) is satisfied. Since $\frac{dx}{dt} < 0$ for $x < x_0$, and $\frac{dx}{dt} > 0$ for $x > x_0$, the fixed point is unstable (Strogatz, 2000).

Even if $x < x_0$, pond growth will be stopped only for a period of time if $\Delta e > 0$. As internal melt reduces the ice density above sea level, surface melting becomes more potent. If the surface density becomes low enough, surface melt could become strong enough to overcome the upward rigid body movement, allowing for pond growth.

It seems unlikely that ponds would actually shrink, as ponded ice melts quickly. Therefore, when $x < x_0$, we expect ponds to stop growing by vertical motion of the topography. In this case it is likely that slower growth by lateral melt would take over, and pond growth could be described by Eq. (26). When $x > x_0$, pond growth by vertical motion of the topography would be possible. It would still be quite slow compared to when Eq. (31) is not satisfied, which means that ponds would likely still grow mostly by lateral melt.

6 Conclusions

We present a simple analytical model for melt pond evolution on permeable Arctic sea ice. The model is represented by two ordinary differential equations in which the rate of change of pond coverage depends on pond coverage. In our model, we reduce a cohort of physical parameters to just four S_{bi}, S_{mp}, S_{bot}, and S_{sm}, which govern the strength of pond growth by bare ice melting, ponded ice melting, ice bottom melting, and vertical sidewall melting. Here, all of the physical parameters combine in a known way, which allows us to assess the behavior of ponds under general conditions. In this way, we find the dependence of pond growth rate on ice thickness, and initial pond coverage. We also find the surprising result that bare ice albedo has a much higher effect on pond coverage than pond albedo. Using the same formalism, we find that in a global warming scenario, pond coverage would change by at least 1.3% per 1 Wm^{-2} of warming per month.

The four modes of growth drive pond evolution in different ways: growth rate due to vertical sidewall melting decreases with pond coverage, growth rate due to ponded ice and ice bottom melting increases with pond coverage, and growth rate due to melting bare ice first increases, and then decreases with pond coverage. Each of these modes leaves a characteristic signature on the pond coverage distribution, so fitting the evolution of pond coverage distribution, instead of fitting the evolution of pond coverage on a single floe, could lead to tighter constraints on the four parameters. The least constrained parameter controls the ice melt near the pond boundary. The rate of ice melt near the pond boundary can significantly affect pond growth, and under certain conditions even prevent it. It follows that a narrow boundary between bare ice and melt ponds can significantly influence the subsequent evolution of the entire ice floe. For this reason it is important that more experiments, field observations, or detailed analysis of the physics at this boundary layer be made.

Acknowledgements. We thank B. Cael Barry, Daniel Koll, Edwin Kite, and Mary Silber for reading the paper and giving useful comments. We also thank Douglas MacAyeal, and Edwin Kite for discussions and ideas about the physical mechanisms involved.

References

Abbot, D. S., Silber, M., and Pierrehumbert, R. T.: Bifurcations leading to summer Arctic sea ice loss, J. Geophys. Res., 116(D19), 2011.

Eicken, H., Grenfell, T. C., Perovich, D. K., Richter-Menge, J. A., and Frey, K.: Hydraulic controls of summer Arctic pack ice albedo, J. Geophys. Res., 109(C8), doi:10.1029/2003jc001989, 2004.

Eisenman, I. and Wettlaufer, J. S.: Nonlinear threshold behavior during the loss of Arctic sea ice, Proceedings of the National Academy of Sciences, 106(1), 28–32, doi:10.1073/pnas.0806887106, 2008.

Flocco, D., and Feltham, D. L.: A continuum model of melt pond evolution on Arctic sea ice, J. Geophys. Res., 112(C8). doi:10.1029/2006jc003836, 2007.

Flocco, D., Feltham, D. L. and Turner, A. K.: Incorporation of a physically based melt pond scheme into the sea ice component of a climate model, J. Geophys. Res., 115(C8), doi:10.1029/2009jc005568, 2010.

Hanesiak, J. M., Barber, D. G., De Abreu, R. A., and Yackel, J. J.: Local and regional albedo observations of arctic first-year sea ice during melt ponding, J. Geophys. Res. Oceans, 106(C1), 1005?1016. doi:10.1029/1999jc000068, 2001.

Holland, M. M., and Bitz, C. M.: Polar amplification of climate change in coupled models, Climate Dynamics, 21(3-4), 221?232. doi:10.1007/s00382-003-0332-6, 2003.

Holland, M. M., Bitz, C. M. and Tremblay, B.: Future abrupt reductions in the summer Arctic sea ice, Geophys. Res. Lett., 33(23), doi:10.1029/2006gl028024, 2006.

Holland, M. M., Bailey, D. A., Briegleb, B. P., Light, B. and Hunke, E.: Improved Sea Ice Shortwave Radiation Physics in CCSM4: The Impact of Melt Ponds and Aerosols on Arctic Sea Ice*, J. Climate, 25(5), 1413–1430, doi:10.1175/jcli-d-11-00078.1, 2012.

Landy, J., Ehn, J., Shields, M., and Barber, D.: Surface and melt pond evolution on landfast first-year sea ice in the Canadian Arctic Archipelago, J. Geophys. Res. Oceans, 119(5), 3054–3075, doi:10.1002/2013jc009617, 2014.

Light, B., Eicken, H., Maykut, G. A., and Grenfell, T. C.: The effect of included participates on the spectral albedo of sea ice, J. Geophys. Res., 103(C12), 27739, doi:10.1029/98jc02587, 1998.

Lüthje, M., Feltham, D. L., Taylor, P. D., and Worster, M. G.: Modeling the summertime evolution of sea-ice melt ponds. J. Geophys. Res., 111(C2). doi:10.1029/2004jc002818, 2006.

Makshtas, A. P. and Podgorny, I. A.: Calculation of melt pond albedos on Arctic sea ice, Polar Research, 15(1), doi:10.3402/polar.v15i1.6635, 1996.

North, G.R.: The Small Ice Cap Instability in Diffusive Climate Models, Journal of the Atmospheric Sciences, 41(23), 3390-3395, 1984.

Nürnberg, D., Wollenburg, I., Dethleff, D., Eicken, H., Kassens, H., Letzig, T., Reimnitz, E. and Thiede, J.: Sediments in Arctic sea ice: Implications for entrainment, transport and release, Marine Geology, 119(3-4), 185–214, doi:10.1016/0025-3227(94)90181-3, 1994.

Pedersen, C. A., Roeckner, E., Lüthje, M. and Winther, J. G.: A new sea ice albedo scheme including melt ponds for ECHAM5 general circulation model, J. Geophys. Res., 114(D8), doi:10.1029/2008jd010440, 2009.

Perovich, D. K., and Polashenski, C.: Albedo evolution of seasonal Arctic sea ice, Geophys. Res. Lett., 39(8), doi:10.1029/2012gl051432, 2012.

Perovich, D. K. and Richter-Menge, J. A.: Loss of Sea Ice in the Arctic*. Annu. Rev. Marine. Sci., 1(1), 417–441. doi:10.1146/annurev.marine.010908.163805, 2009.

Perovich, D. K., Roesler, C. S., and Pegau, W. S.: Variability in Arctic sea ice optical properties, J. Geophys. Res., 103(C1), 1193, doi:10.1029/97jc01614, 1998.

Perovich, D. K., Grenfell, T. C., Light, B., and Hobbs, P. V.: Seasonal evolution of the albedo of multiyear Arctic sea ice, J. Geophys. Res., 107(C10). doi:10.1029/2000jc000438, 2002b.

Perovich, D. K., Thomas, C. G., Richter-Menge, J. A., Light, B., Tucker, W. B., and Eicken, H.: Thin and thinner: Sea ice mass balance measurements during SHEBA, J. Geophys. Res., 108(C3), doi:10.1029/2001jc001079, 2003.

Perovich, D. K., Light, B., Eicken, H., Jones, K. F., Runciman, K. and Nghiem, S. V.: Increasing solar heating of the Arctic Ocean and adjacent seas, 1979–2005: Attribution and role in the ice-albedo feedback, Geophys. Res. Lett., 34(19), doi:10.1029/2007gl031480, 2007.

Pfirman, S., Lange, M. A., Wollenburg, I. and Schlosser, P.: Sea Ice Characteristics and the Role of Sediment Inclusions in Deep-Sea Deposition: Arctic — Antarctic Comparisons, Geological History of the Polar Oceans: Arctic versus Antarctic, 187–211, doi:10.1007/978-94-009-2029-3_11, 1990.

Polashenski, C., Perovich, D., and Courville, Z.: The mechanisms of sea ice melt pond formation and evolution, J. Geophys. Res., 117(C1). doi:10.1029/2011jc007231, 2012.

Raymond, C. F., and Tusima, K.: Grain coarsening of water-saturated snow, Journal of Glaciology, 22(86), 83-105, doi:10.3198/1979JoG22-86-83-105, 1979.

Scott, F. and Feltham, D. L.: A model of the three-dimensional evolution of Arctic melt ponds on first-year and multiyear sea ice, J. Geophys. Res., 115(C12), doi:10.1029/2010jc006156, 2010.

Screen, J. A. and Simmonds, I.: The central role of diminishing sea ice in recent Arctic temperature amplification, Nature, 464(7293), 1334–1337, doi:10.1038/nature09051, 2010.

Serreze, M. C., and Stroeve, J.: Arctic sea ice trends, variability and implications for seasonal ice forecasting, Phil. Trans. R. Soc. A, 373(2045), 20140159, doi:10.1098/rsta.2014.0159, 2015.

Skyllingstad, E.D., Paulson, C.A. and Perovich, D.K.: Simulation of melt pond evolution on level ice. J. Geophys. Res.: Oceans, 114(C12). doi:10.1029/2009jc005363, 2009.

Stroeve, J., Holland, M. M., Meier, W., Scambos, T. and Serreze, M.: Arctic sea ice decline: Faster than forecast, Geophys. Res. Lett., 34(9), doi:10.1029/2007gl029703, 2007.

Strogatz, S. H.: Nonlinear dynamics and chaos with applications to physics, biology, chemistry, and engineering, Westview Press, Cambridge, MA., 2000.

Tucker, W. B., Gow, A. J., Meese, D. A., Bosworth, H. W. and Reimnitz, E.: Physical characteristics of summer sea ice across the Arctic Ocean, J. Geophys. Res., 104(C1), 1489–1489, doi:10.1029/98jc02607, 1999.

Taylor, P. D., and Feltham, D. L.: A model of melt pond evolution on sea ice, J. Geophys. Res. Oceans, 109(C12). doi:10.1029/2004jc002361, 2004.

Webster, M. A., Rigor, I. G., Perovich, D. K., Richter-Menge, J. A., Polashenski, C. M., and Light, B.: Seasonal evolution of melt ponds on Arctic sea ice, J. Geophys. Res. Oceans, 120(9), 5968–5982, doi:10.1002/2015jc011030, 2015.

Yackel, J. J., Barber, D. G. and Hanesiak, J. M.: Melt ponds on sea ice in the Canadian Archipelago: 1. Variability in morphological and radiative properties, J. Geophys. Res., 105(C9), 22049–22049, doi:10.1029/2000jc900075, 2000.

Zhang, J., Lindsay, R., Steele, M. and Schweiger, A.: What drove the dramatic retreat of arctic sea ice during summer 2007?, Geophys. Res. Lett., 35(11), doi:10.1029/2008gl034005, 2008.

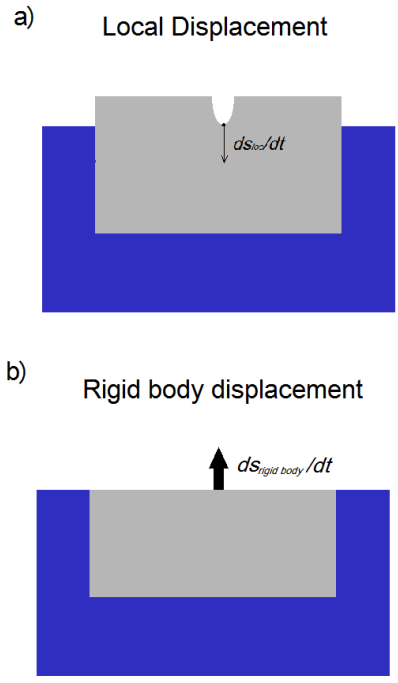

Figure 1. a) Local displacement represents the movement of a point on the ice surface as a result of ice melting at that particular point. It is a function only of local ice characteristics at that point. For both local and hydrostatic displacements the positive direction is defined as upwards. b) Hydrostatic adjustment represents the motion of a floe as a whole in an effort to maintain hydrostatic balance because melting removes mass above or below sea level. Melting above sea level induces an upward motion of the floe, whereas melting below sea level induces a downward motion.

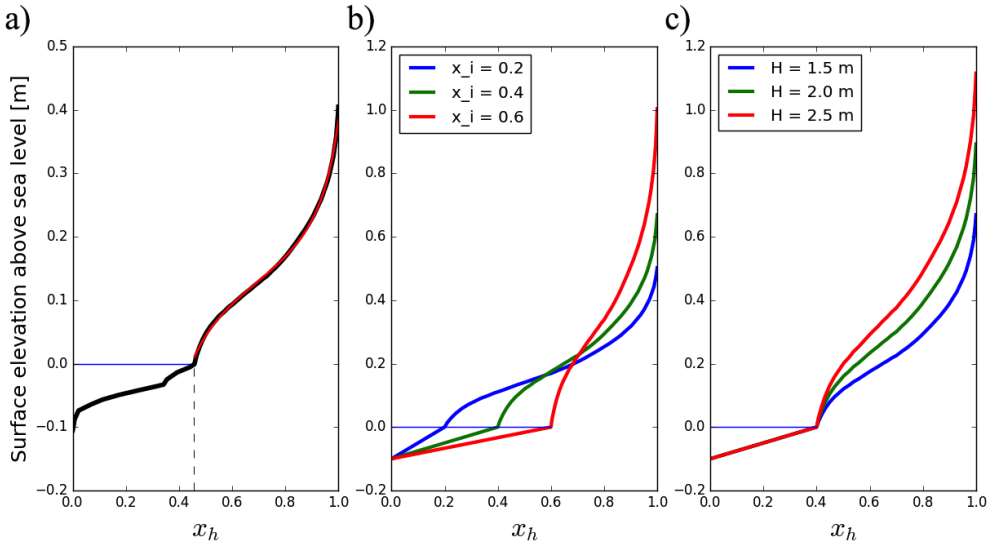

Figure 2. Hypsographic curves show the percentage of the sea ice surface that is lower than a particular elevation. Pond coverage on highly permeable sea ice can be inferred from here as an intersection of sea level (horizontal blue line) with the hypsographic curve. a) Hypsographic curve measured by Landy et. al. (2014) for June 25th of 2011. The vertical dashed line represents the pond coverage, assuming that ice is permeable enough. The red line represents a fit to the part of the hypsographic curve above sea level with a function $s(x_h) = a\tan(bx_h + c) + d$. b) Three hypsographic curves for different initial pond coverage, and the same ice thickness. c) Three hypsographic curves for the same initial pond coverage, and different ice thickness.

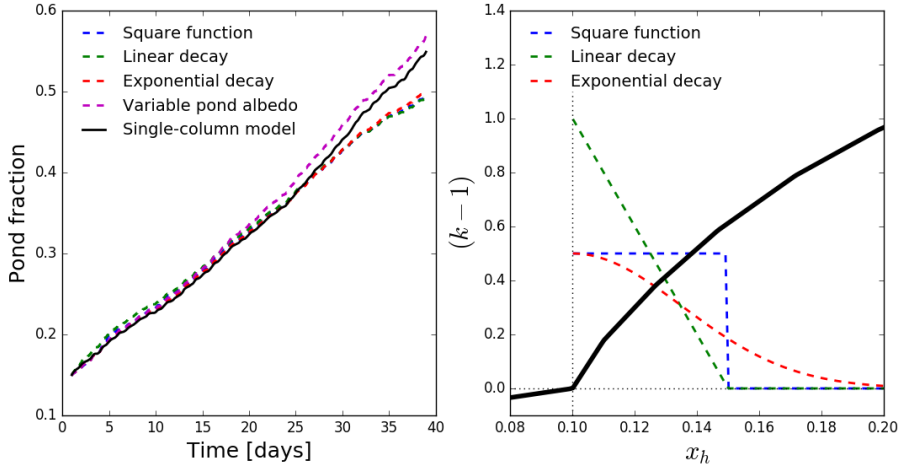

Figure 3. a) A comparison between pond evolution in the simple model and the 1D model. Solid black curve represents the simple model. The dashed blue, green, and red lines represent the 1D model for different functions $k(x_h)$ shown in panel b). These different functions were chosen such that the integral parameter $K = \int (k(x_h) - 1) dx_h$ is the same as for the simple model. The dashed magenta curve represents the 1D model with pond albedo varying with depth. There is significant agreement between all the curves, suggesting that the simplifications made in the simple model were justified. Since including the variable pond albedo does not change the pond evolution significantly, this detail can most likely be ignored when estimating the pond coverage on permeable ice. b) Dashed blue, green, and red lines represent functions $k(x_h) - 1$ used to run the 1D model. Thick black line represents the hypsographic curve near the pond edge.

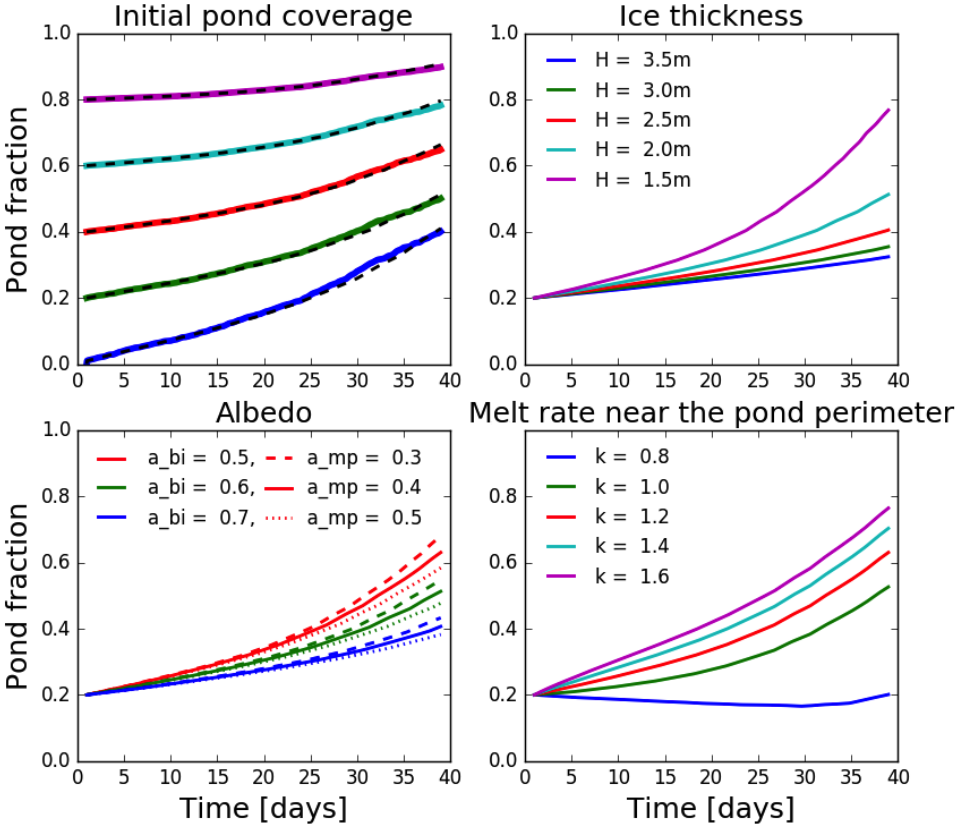

Figure 4. Numerical solutions to Eq. (21) using varying parameters around the defaults described in the text. a) Varying initial pond coverage. Solid lines represent solutions using full time-varying fluxes, while dashed lines represent solutions using time-averaged fluxes. The two solutions are very similar, and for this reason we subsequently use only the time-averaged fluxes. b) Varying ice thickness. Ponds grow slower on thicker floes. c) Varying pond and bare ice albedo. Different colors represent different bare ice albedo, and full, dotted, and dashed lines represent different pond albedo. A change in bare ice albedo has a much larger effect on pond fraction than the same change in pond albedo. d) Varying the constant k. For $k = 0.8$, the ponds shrink. However, pond evolution for $k < 1$ is not represented well in our model, so this curve serves only as an illustration.

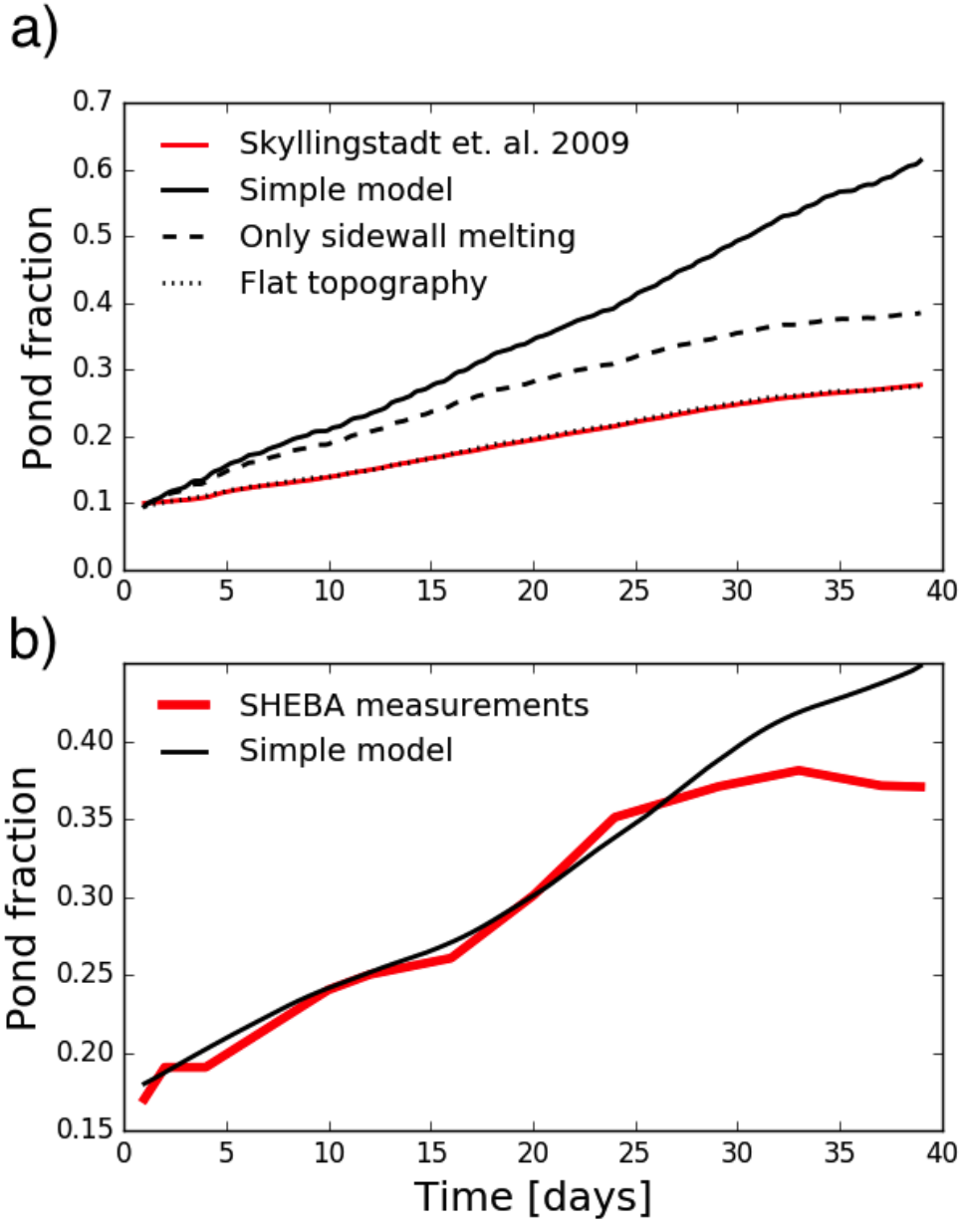

Figure 5. a) A comparison between different variations of our model. The red line is the results of Skyllingstad et. al. (2009). The dashed line represents our model with only vertical sidewall melting included. The dotted line represents only vertical sidewall melting using a flat topography. The full line represents our model when freeboard sinking is included. b) A comparison between measurements of pond fraction made during SHEBA along the albedo line (red line), and our model (black line).

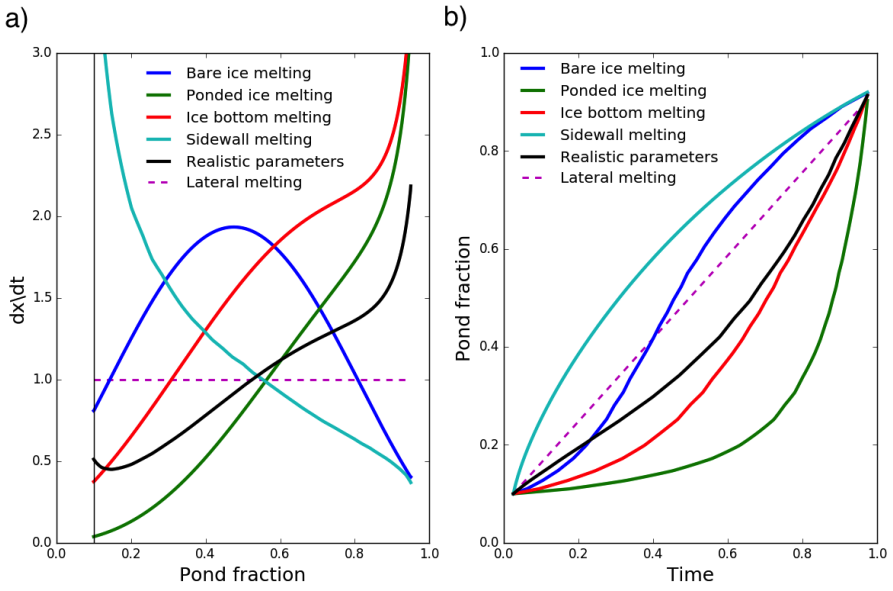

Figure 6. a) Phase portraits for different modes of pond growth. The growth rate for each of the growth modes is normalized for visual clarity. Pond growth rate for bare ice melting (blue line) first increases up to a certain pond coverage that lays roughly at the midpoint between x_i and 1, and decreases afterwards. Ponded ice melting (green line), and ice bottom melting rates (red line) both increase with pond coverage. Vertical sidewall melting rate (cyan line) decreases with pond coverage. The black line represents a realistic combination of the four growth modes, and shows a slowly increasing pond growth rate over much of the phase space. The dashed magenta line represents lateral melting. b) Solutions to Eq. (21) when only one of the growth modes is active. The time axis is normalized for visual clarity.

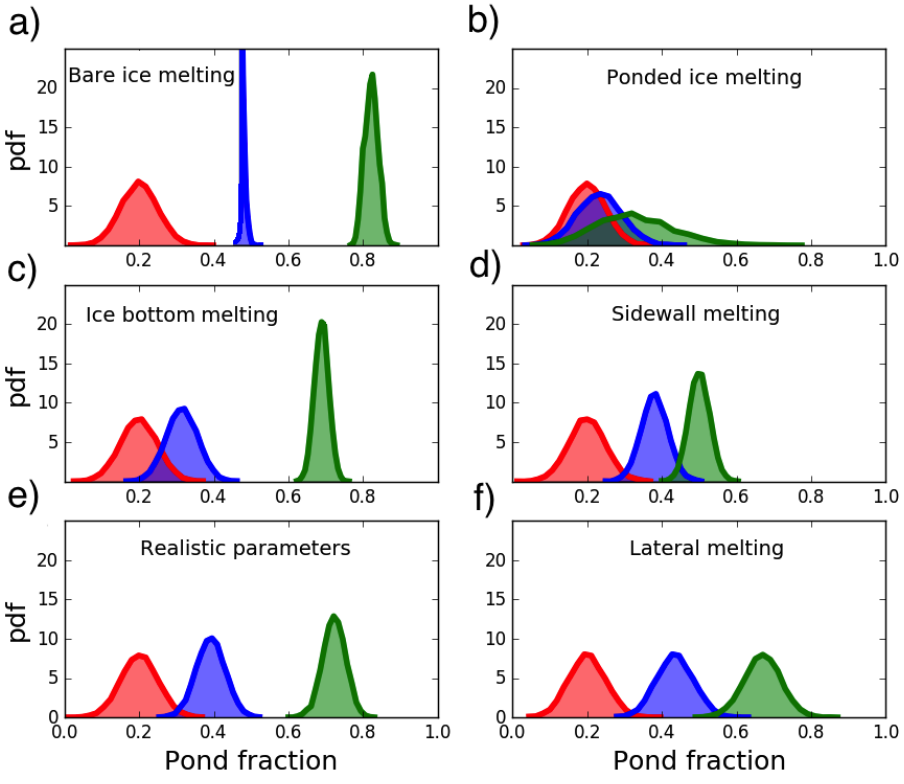

Figure 7. In this figure we have evolved an ensemble of 10^5 floes with varying initial pond coverage according to Eq. (21) when only one of the growth modes is active. Red curves represent the initial pond fraction distribution, blue curves represent the pond fraction distribution after 25 days, while the green curves represent the pond fraction distribution after 50 days. We show how different growth modes have differing effects on the pond fraction distribution. a) Bare ice melting first narrows the distribution, and then widens it. b) Ponded ice melting widens the distribution. c) Bottom ice melting narrows the distribution, while the mean of the distribution increases at an increasing rate. d) Vertical sidewall melting narrows the distribution, while the mean of the distribution increases at a decreasing rate. e) Using realistic parameters, the pond distribution slowly narrows and accelerates. f) If there exists a physical fixed point, $0 < x_0 < 1$, ponds likely grow via lateral melting. In this way, pond coverage distribution does not change width, and the growth is linear.